

LANDSLIDE INVESTIGATION WITH THE USE OF GEOPHYSICAL METHODS: A CASE STUDY IN NORTHEASTERN TURKEY

Kenan Gelisli^{1*}, Hakan Ersoy²

¹Department of Geophysics, Karadeniz Technical University, Trabzon, Turkey

²Department of Geology, Karadeniz Technical University, Trabzon, Turkey

Abstract. The authors of this paper examined the structure of the Havuzlu Paleo-Landslide which is in the reservoir area of the ongoing construction of Artvin Dam and Hydroelectric Power Plant (Yusufeli-Artvin, Northeastern Turkey). The toe of the Havuzlu Landslide will be in the dam reservoir lake area with water accumulation. This may trigger a landslide, which could be a threat to the dam. Geophysical methods were used to delineate the geometry of the Havuzlu Landslide in the dam reservoir area. The 2D electric resistivity imaging surveys in the studied area were conducted along 22 profiles, and Self-Potential measurements were also performed along 11 resistivity lines. In addition, microtremor measurements were taken on 16 points of the Havuzlu slope. Sixteen boreholes varying in depth from 40 to 120 meters were also drilled for analyzing the structure of the subsurface, groundwater conditions and geotechnical properties. The structure of the Havuzlu Landslide was determined with boreholes and geophysical measurements. Anomalies in the groundwater movement were observed using the Self-Potential method and the borehole data. Geophysical data showed compatibility with borehole data.

Keywords: *Havuzlu Landslide (Northeastern Turkey), geophysical methods, landslide structure.*

Corresponding Author: Prof. Dr. Kenan Gelisli, Department of Geophysics, Karadeniz Technical University, 61080 Trabzon, Turkey, e-mail: gelisli@ktu.edu.tr

Manuscript received: 13 February 2017

1. Introduction

Landslide is the downward moving of a slope caused by geological, geomorphological, hydrological factors and seismicity. Landslides are one of the natural disasters which affect both humans and natural environment. Large-scale landslides in dam areas threaten the safety of the dams.

The Artvin Dam and Hydroelectric Power Plant, which will produce 332 MW per year, is located in the middle Çoruh basin in the Northeastern Turkey (Figure 1). The slopes in the reservoir area are usually steep and have many narrow defiles. The Havuzlu Landslide is located within the boundaries of Havuzlu Village, which is located in the reservoir basin of the Artvin Dam and Hydroelectric Power Plant. When the reservoir of the dam is filled with water, Havuzlu Landslide, which can be damage Havuzlu Village and Artvin Dam, can be affected.

Landslides frequently occur in several areas in the Northeast Turkey due to geomorphological structures and excessive rainfall. The landslide problem, which is very important for the region, has been investigated by many researchers since 1950's [6, 16, 43, 44, 54, 10, 14, 57, 2, 3, 41, 12].

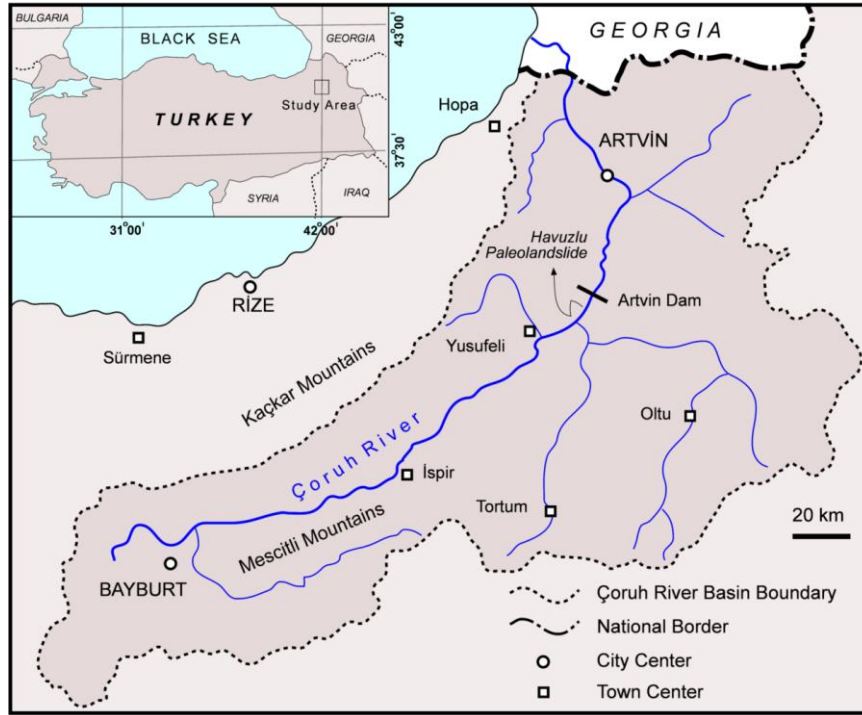


Figure 1. Location map of the study area.

Geophysical methods are used to determinate the structure of the landslide and its lateral extent and the depth to the failure surface [39, 11, 19, 27, 32, 31, 7, 23, 17, 28, 37, 49, 21, 46]. These methods are also used to investigate the hydrogeological problems in the slope [9, 38, 33, 8]. Perrone et al., studied the Varco d'Izzo landslide (Basilicata region, Italy) with 2-D electrical resistivity method and the data from three direct boreholes [46]. Electrical resistivity and seismic refraction tomography results obtained from Altındag landslide area (Izmir, Turkey) were compared by Göktürkler et al., [24]. The 3D fence diagram of all resistivity data acquired along parallel profiles in a landslide located on the Quesnel River in British Columbia (Canada) were made by Bichler et al., [7]. Self-Potential (SP) measurements provide information about the movement of groundwater [56, 36, 52, 55, 15, 1, 29, 30]. Microtremor method is used mostly in earthquake engineering to determinate the underground geometry and shear wave velocities [40, 13, 5, 48].

The 2D resistivity surveys in the studied area were carried out to outline the geometries of the Havuzlu Landslide along 22 profiles. The underground 2D resistivity distribution was calculated with the inverse transform of the measured 2D resistivity data [35]. SP measurements were also made along 11 resistivity lines. In addition, microtremor measurements were taken on 16 points of the slope. Sixteen boreholes were drilled for analyzing the structure of the subsurface, groundwater conditions and geotechnical properties. All drillings ended after a few meters advance into the bedrock. Detailed information of the boreholes is given in Table 1.

Table 1. Information about the boreholes in the study area. YSK-1, 2, 3, 4, 5, 6, 7, 8, HSK-4, 5, 6: ground investigation boreholes, INK-1: Inclinometer borehole, P-1, 2, 3, 4: pressuremeter test boreholes and YSK-9: abandoned well.

Sounding No	Coordinates		Kot (m)	Rock depth (m)	Rock Elevation (m)	Total Depth (m)
	Y	X	Z			
YSK-1	475006.06	4529244.17	1078.596	39.00	1039.6	75.00
YSK-2	475226.43	4528947.02	929.036	86.00	843.04	97.10
YSK-3	475332.42	4528785.29	848.029	80.80	767.23	91.80
YSK-4	475471.89	4528447.80	698.754	83.00	615.75	100.00
YSK-5	475532.83	4528348.61	664.345	105.00	559.35	117.50
YSK-8	475764.67	4528234.44	523.031	33.00	490.03	51.00
YSK-9	475438.00	4528563.78	739.000	-	-	80.20
YSK-10	475623.77	4528502.37	679.617	78.00	601.62	93.60
INK-1	475597.52	4528436.22	670.941	69.00	601.94	88.00
P-1	475761.86	4528259.34	538.914	41.00	497.91	50.00
P-2	474697.40	4528228.22	556.858	44.00	512.86	60.00
P-3	475708.90	4528327.12	598.770	55.30	543.47	70.00
P-4	475781.74	4528363.14	574.533	40.00	534.53	60.00
HSK-4	475695.09	4528200.00	550.787	62.00	488.78	76.50
HSK-5	475737.31	4528326.00	586.238	61.00	525.23	85.00
HSK-6	475821.51	4528395.00	578.47	40.00	538.47	61.00
Total						1257.7

The engineering properties of the cores, which were taken from boreholes, were investigated with laboratory tests. Inclinometer and groundwater level measurements were performed on one of the wells. Furthermore, another four wells were used for pressuremeter tests. The studies on the data obtained from the boreholes and laboratory tests are still continues.

The results of geophysical investigations were systematically integrated with the data collected from geological and morphological observations and borehole applications. The sliding surface of Havuzlu Landslide and the groundwater condition were determined with the joint interpretation of geological and geophysical data.

2. Geological setting

The Eastern Pontide located at the mountain chain having 500 km long and 100 km wide is main metallogenetic province in the coastal region of the southern east Black Sea. Considering its structural and lithological differences, this province was subdivided into two different zones, northern and eastern [45, 42]. Late Cretaceous and Middle Eocene volcanic rocks are main lithological units in the other zone [4, 51].

The studied site is located at the northern zone of the eastern Pontides consists of Paleozoic-Triassic magmatic complex (Demirkent Magmatic Complex), Jurassic granitic intrusions (Sebzeciler Granodiorite), metamorphics (Berta Formation), volcanic rocks (Mudurnu Formation), and Quaternary unconsolidated lithologies (Figure 2).

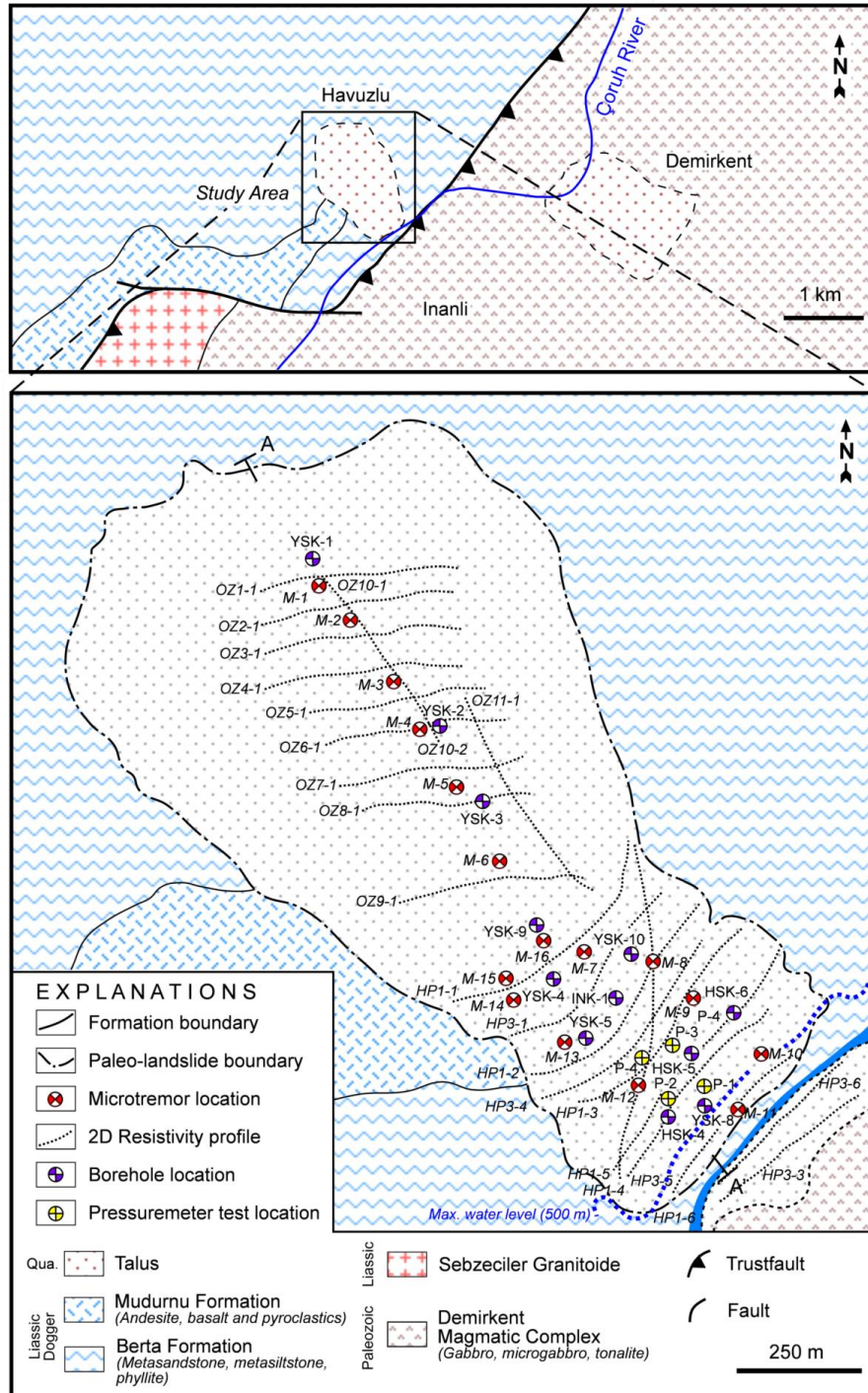


Figure 2. General geology map of the study area and location of the 2D electrical resistivity profiles, microtremor stations, and boreholes.

The dominant lithologies around the studied paleo-landslide area are basaltic, andesitic volcanic rocks in Mudurnu Formation and metasandstones, and metasiltsstones in Berta Formations. The landslide contains clay, silt, sand, gravel, and block-size materials. In other words, mega-blocks (5-6 m diameters) are

observed in the landslide materials. These materials generally consist of metasandstones, metasiltsstones, and rarely andesites and basalts. The thickness of the landslide materials is greater than 100 m in some places in field.

3. Geophysical studies

The resistivity survey aims to determine the resistivity distribution in the subsurface by making measurements along the ground surface. It is based on measuring the electrical potential between a pair of electrodes caused by direct current injection between another pair of electrodes. Afterwards, the apparent resistivity is calculated using the geometric factor. For field practice different electrode configurations have been designed.

The electrical resistivity imaging method is an active geoelectrical prospecting technique used to obtain a high-resolution image of the subsurface electrical resistivity. The 2D electrical resistivity imaging technology is a combination of vertical electrical sounding and resistivity profile measurement techniques. It has been used to identify the discontinuity between the landslide material and the bedrock [28]. 2D data are generally presented in the form of a pseudo section, which is a representation of the apparent resistivity variations in the subsurface. Resistivity distribution of the underground is obtained from the 2D inversion of apparent resistivity data [35]. The electric resistivity values of rocks vary in a wide range and its depend on a grain size, porosity, contents of water and mineralization of the rocks.

SP Method investigates the natural potential variations in the field with by using the measurements obtained with non-polarized electrode combinations. It is found by in situ experiments that self-voltage also originates from underground water flow along with some other factors. For this reason, the SP method is used to determine existing groundwater flows on landslide investigations. Observed high negative SP anomalies indicate the existence of groundwater flow.

The engineering properties of the soil of site are investigated with microtremor methods. The microtremor survey method listens to the natural and unnatural signals and analyzes for subsurface acoustic properties, in particular the shear-velocity profile for the earth at a scale of a few kilometers. The required instrumentation is simple and can be applied where conventional seismic surveying is difficult, particularly in urban areas [53]. A lot of researchers used this method to determinate the thickness and the natural frequency of soft sediments [40, 20, 34]. The observed single station microtremor signals are analyzed by the Fast Fourier Transform Method (FFT) [26]. The bedrock depths of the Havuzlu Landslide were computed with microtremor method observed at the landslide body by using the horizontal to vertical component spectral ratio (H/V Nakamura technique).

We collected a 2D resistivity data along the 22 profiles over the Havuzlu Landslide area using a multi electrode system in a dipole-dipole gradient array with an electrode spacing of 20 m (Figure 2). Profiles were generally oriented perpendicular and only two were parallel to the landslide body. According to the electrode spacing at all these profiles, the depths of geological structures were

estimated to be over 100 m. The 2D electrical resistivity data were analyzed using the EarthImager 2D software. The horizontal and vertical subsurface cross-sections for the Havuzlu slope were prepared from the 2D inversions of the measured resistivity data. The computed 2D electrical resistivity images of the HP1.3 and HP1.5 profiles are shown in Figure 3.

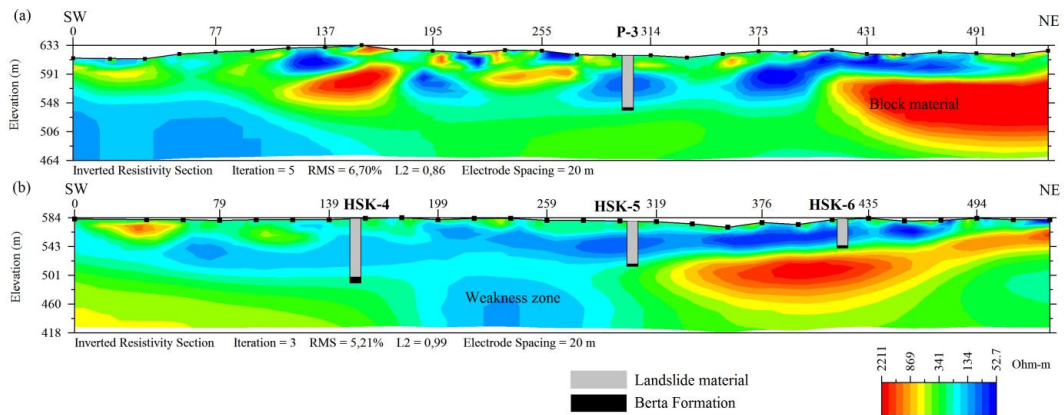


Figure 3. 2D electrical resistivity imaging of the HP1.3 profile (a) and HP1.5 profile (b) of the Havuzlu Landslide compared to the stratigraphic data from boreholes P-3, HSK-4, HSK-5, and HSK-6.

The boreholes, which are close to the cross sections, are also shown in this figure. The underground 2D resistivity sections illustrate an extremely heterogeneous structure both vertically and horizontally. The length of these lines was about 500 m, and they were oriented perpendicular to the landslide body. There are low and high resistivity zones in these sections. Underground resistivities vary to the large-scales. Zones of relatively low resistivities within the body of landslide are described with content of clayey, silty, sandy materials and moisture contents. The landslide body includes large block rock materials. The cores obtained from the HSK-5 boreholes are shown in Figure 4.



Figure 4. View of the cores obtained from the HSK-5 borehole.

Clayey, silty, and sandy material and massive samples can be clearly seen in this figure. The computed underground 2D resistivity distribution and borehole data showed a good correlation. The relatively high resistivity zones of these sections correspond to the block materials in the landslide body and massive bedrock formations. Low resistivities, which are located in the bedrock, are identified as moistured and fractured zones. The resistivities of the bedrock are higher than 115 Ohm-m when compared with the boreholes cores and the calculated resistivities. Therefore, the values which are about 115 Ohm-m and higher, calculated in 2D resistivity sections are accepted as Berta Formations.

The SP measurements were also performed along 11 lines for determining the presence of groundwater movement. The SP data indicate groundwater movement in some regions. The SP data obtained from some part of the HP1.1 profile is shown in Figure 5. The anomalies above -20 mV are observed in some locations (Figure 5). Groundwater measurements taken from the wells were encountered poor ground water movement in the areas close to the bedrock contact.

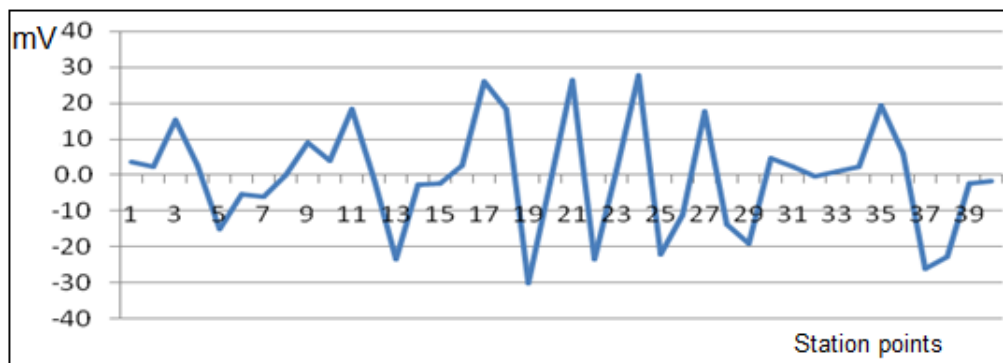


Figure 5. The SP graph collected from some part of the HP1.1 profile. Observed high negative SP anomalies indicate the existence of groundwater flow.

To correlate depths found from resistivity method and boreholes, 16 seismic microtremor sounding measurements were also carried out (Figure 2). Firstly, the good quality data windows for every station were chosen from the microtremor measurements. Additionally, spectral ratios H/V (Horizontal spectrum/Vertical spectrum) were calculated for each point, and predominant frequencies of soil were designated. For computation of the spectral ratios using Nakamura's method, the SESAME software was used [18]. The computed H/V ratios for 20 windows selected from three components of the microtremor records collected from the M-13 point are shown in Figure 6. The depths of bedrock were calculated by empiric formulae that included the soil frequency. The depths calculated from this method were found to be different from resistivity section and borehole data comparatively.

Failure surface is determined with the results of the resistivity method and the borehole data. The cross-section A-A' (location in Figure 2) which is formed from the axis of the Havuzlu Landslide by using the depth obtained from the

resistivity method and boreholes is shown in Figure 7. The 2D resistivity depth values and borehole results evidently support each other. The thickness of the Havuzlu Landslide body, which is higher in its middle parts, varies between 39 m and 105 m.

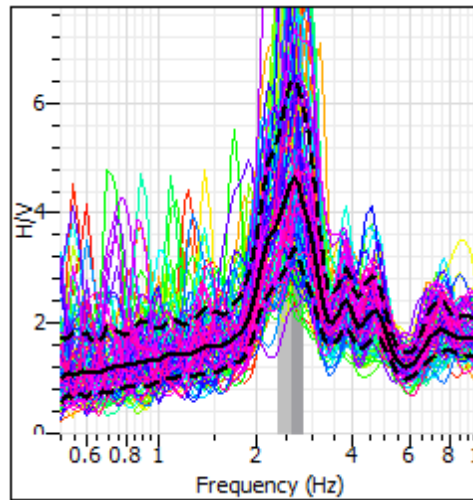


Figure 6. An example of the H/V (Horizontal spectrum/Vertical spectrum) selected for 20 windows obtained from the M-13 point three component microtremor records.

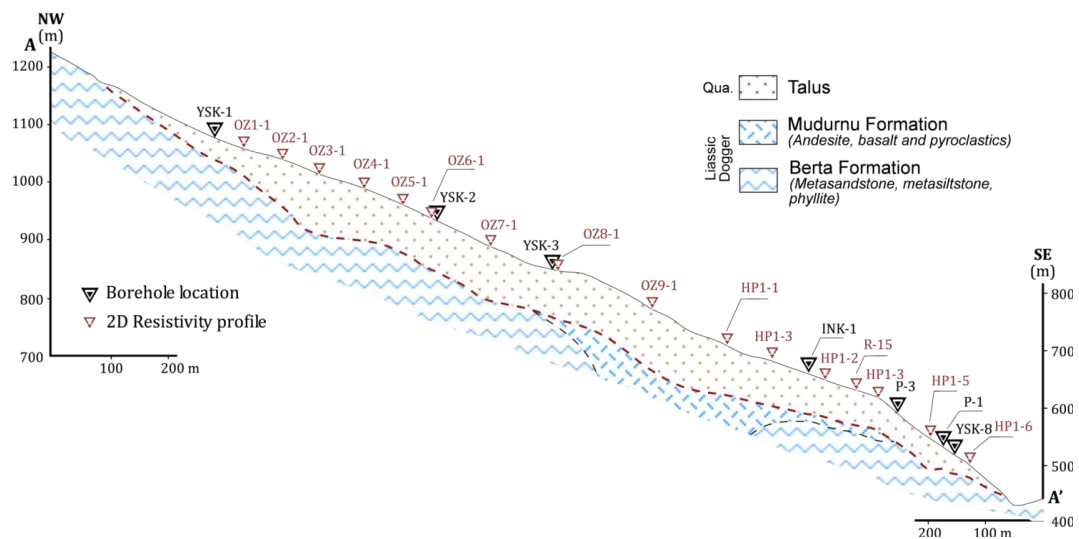


Figure 7. (A-A') Geological cross-section (location in Figure 2) formed from electrical resistivity and borehole data.

4. Discussion and conclusions

In this study, the structure of the Havuzlu Landslide and the groundwater condition were investigated to calculate the stability of the slope. The Havuzlu Landslide material consists of coarse-grained material with very low cohesion, mostly blocky, with little silty-clayey sand. A total of 1257,7 m drilling holes were drilled in the Havuzlu slope. Observations of groundwater and inclinometer and pressiometry measures in the boreholes have been taken and some measurements are ongoing. The geophysical data were successfully used for the interpretation of the spatial structure of the Havuzlu Landslide. The geophysical data were interpreted with using both geological and borehole data. The 2D electrical resistivity images with relatively low resistivity contrasts between the disturbed and the undisturbed mass outlined the geometry and boundaries of the investigated landslide. The geoelectrical study revealed the zones with a content of clayey, silty, sandy material, moist areas and massive blocks. And resistivity sections also revealed that at some places the bedrock is cracked and fractured. The depth of sliding surface was determined from resistivity, microtremor measurements, and borehole data. These studies have shown the minimum and maximum depths of the landslide material to be between 39 and 105 meters, respectively. The presence of weak water movement at close the bedrock was detected using SP data and the groundwater measurements in the boreholes. The results of the laboratory tests showed the landslide material with more sand and gravel, less silt and clay has low cohesion and high internal friction angle. In some places, the depth of the bedrock obtained from microtremor data is incompatible with those obtained from the wells. The structure of the Havuzlu slope was determined in combination with boreholes data and geophysical measurements. Safety factor will also be calculated with using the geotechnics and laboratory data.

Acknowledgements

This work was financially supported by Doğu Energy A.Ş.. Special thanks to all the people who participated to the field investigation.

References

1. Abdelrahman E., Soliman K., Abo-Ezz E., et al., (2009) Quantitative interpretation of self-potential anomalies of some simple geometric bodies, *Pure Appl. Geophysics*, 166, 2021–2035.
2. Akgun A., Bulut F., (2007) GIS based landslide susceptibility for Arsin-Yomra (Trabzon, North Turkey) region, *Environmental Geology*, 51(8), 1377-1387.
3. Akgun A., Dag S., Bulut F., (2008) Landslide susceptibility mapping for a landslide-prone area (Findikli, NE of Turkey) by likelihood-frequency ratio and weighted linear combination models, *Environmental Geology*, 54, 1127-1143.

4. Arslan M., Tuysuz N., Korkmaz S., et al., (1997) Geochemistry and petrogenesis of the eastern Pontide volcanic rocks, Northeast Turkey, *Chemie der Erde*, 57, 157–187.
5. Bard P.Y., (1999) Microtremor measurements: a tool for site effect estimation. in Proceedings of the Second International Symposium on the Effects of Surface Geology on Seismic Motion, Yokohama, Japan, December 1–3, 3, 1251–1279.
6. Beret B., (1955) Sera Heyelanı, *Türkiye Coğrafya Dergisi*, 13-14.
7. Bichler A., Bobrowsky P., Best M., et al., (2004) Three-dimensional mapping of a landslide using multi-geophysical approach: The Quesnel Forks landslide, *Landslides*, 1, 29-40.
8. Bièvre G., Jongmans D., Winiarski T., et al., (2012) Application of geophysical measurements for assessing the role of fissures in water infiltration within a clay landslide (Trieves area, French Alps), *Hydrol. Process*, 26, 2128–2142.
9. Bruno F., Marillier F., (2000) Test of high-resolution seismic reflection and other geophysical techniques on the Boup landslide in the Swiss Alps, *Surveys in Geophysics*, 21(4), 333-348.
10. Bulut F., Boynukalın S., Tarhan F., Ataoglu E., (1999) Reliability of landslide isopleth maps, *Bulletin of Engineering Geology and the Environment*, 58, 95-98.
11. Cummings D., Clark BR., (1998) Use of seismic refraction and electrical resistivity surveys in landslide investigations, *Bulletin of the Association of Engineering Geologists*, 25(4), 459-464.
12. Dag S., Bulut F., (2012) Coğrafi bilgi sistemleri tabanlı heyelan duyarlılık haritalarının hazırlanmasına bir örnek: Cayeli (Rize, KD Turkey), *Jeoloji Mühendisliği Dergisi*, 36(1), 35-62.
13. Dowrick D.J., (1997) Earthquake Resistant Design for Engineers and Architects (Second Ed.), John Wiley & Sons.
14. Duman T.Y., Nefeslioglu H.A., Can T., Olgun Ş., Durmaz S., Hamzacebi S., Coreklioglu Ş., (2007) Türkiye heyelan envanter haritaları, 58. Türkiye Jeoloji Kurultayı, p.326.
15. El-kaliouby H., Al-Garni M., (2009) Inversion of self-potential anomalies caused by 2d inclined sheets using neural networks, *J. Geophys. Eng.*, 6, 29–34.
16. Erguvanlı K., Tarhan F., (1982) Doğu Karadeniz kıyı şeridindeki kütle hareketlerinin mühendislik jeolojisi açısından değerlendirilmesi, *KTÜ Yer Bilimleri Dergisi*, 100. Yıl özel sayı.
17. Friedel S., Thielen A., Springman S.M., (2006) Investigation of a slope endangered by rainfall-induced landslides using 3D resistivity tomography and geotechnical testing, *Journal of Applied Geophysics*, 60, 100-114.
18. Galgaro A., Boaga J., Rocca M., (2014) HVSR technique as tool for thermal-basin characterization: a field example in N-E Italy, *Environ. Earth Sci.*, 71, 4433–4446.
19. Gallipoli M., Lapenna V., Lorenzo P., Mucciarelli M., Perrone A., Piscitelli S., Sdao F., (2000) Comparison of geological and geophysical prospecting

- techniques in the study of a landslide in southern Italy, *Eur. J. Env. Eng. Geophys.*, 4, 117-128.
20. Garcia-Jerez A., Luzon F., Navarro M., Perez-Ruiz J.A., (2006) Characterization of the sedimentary cover of the Zafarraya Basin, Southern Spain, by means of ambient noise, *Bull Seismol Soc Am.*, 96, 957–967.
 21. Gelisli K., Seren A., Babacan A.E., Çatakli A., Ersoy H., Kandemir R., (2011) The Sumela Monastery slope in Maçka, Trabzon, northeast Turkey: rock mass properties and stability assessment, *Bulletin of Engineering Geology and the Environment*, 70, 577-583.
 22. Giano S.I., Lapenna V., Piscitelli S., Schiattarella M., (2000) Electrical imaging and self-potential surveys to study the geological setting of the Quaternary slope deposits in the Agri high valley (southern Italy), *Annali di Geofisica*, 43, 409–419.
 23. Godio A., Strobbia C., De Bacco G., (2006) Geophysical characterization of a rockslide in an alpine region, *Engineering Geology*, 83, 273–286.
 24. Göktürkler G., Balkaya C., Erhan Z., (2008) Geophysical investigation of a landslide: The Altındağ landslide site, İzmir (western Turkey), *Journal of Applied Geophysics*, 65, 84-96.
 25. Griffiths D.H., Barker R.D., (1993) Two-dimensional resistivity imaging and modelling in areas of complex geology, *Journal of Applied Geophysics*, 29, 211–226.
 26. Guo M.Z., Ren F.H., (2005) The microtremor methods for dynamics measurement of sites, *World Earthquake Engineering*, 21(4), 139-142.
 27. Hack R., (2000) Geophysics for slope stability, *Surv. Geophysics*, 21, 423-448.
 28. Jongmans D., Garambois S., (2007) Geophysical investigation of landslides: a review, *Bull. Soc. Geol. Fr.*, 178(2), 101-112.
 29. Jouniaux L., Mainault A., Naudet V., et al., (2009) Review of self-potential methods in hydrogeophysics, *C. R. Geoscience*, 341, 928–936.
 30. Jouniaux L., Ishido T., (2012) Electrokinetics in Earth Sciences: a tutorial, *Int. J. Geophysics*, (Hindawi Publishing Corporation), Article ID 286107.
 31. Israil M., Pachauri A.K., (2003) Geophysical characterization of a landslide site in the Himalayan foothill region, *Journal of Asian Earth Sciences*, 22, 253–263.
 32. Lapenna V., Lorenzo P., Perrone A., Piscitelli S., Sdao F., Rizzo E., (2003) High-resolution geoelectrical tomographies in the study of Giarrossa landslide (southern Italy), *Bulletin of Engineering Geology and the Environment*, 62, 259–268.
 33. Lapenna V., Lorenzo P., Perrone A., Piscitelli S., (2005) 2D electrical resistivity imaging of some complex landslides in the Lucanian Apennine chain, southern Italy, *Geophysics*, 70(3), 11-18.
 34. Le Roux O., Cornou C., Jongmans D., Schwartz S., (2012) 1-D and 2-D resonances in an Alpine valley identified from ambient noise measurements and 3-D modeling, *Geophys J Int.*, 191(2), 579-590.

35. Loke M.H., Barker R.D., (1996) Rapid least-squares inversion of apparent resistivity pseudosections by a quasi-Newton method, *Geophysical Prospecting*, 44, 131-152.
36. Maineult A., Jouniaux L., Bernab e Y., (2006) Influence of the mineralogical composition on the self-potential response to advection of kcl concentration fronts through sand, *Geophys. Res. Lett.*, 33, L24311.
37. Marescot L., Monnet R., Chapellier D., (2008) Resistivity and induced polarization surveys for slope instability studies in the Swiss Alps, *Engineering Geology*, 98, 18-28.
38. Mauritsch H.J., Seiberl W., Arndt R., Romer A., Schneiderbauer K., Sendlhofer G.P., (2000) Geophysical investigations of large landslides in the Carnic region of southern Austria, *Engineering Geology*, 56(3-4), 373-388.
39. Mc Cann D.M., Forster A., (1990) Reconnaissance geophysical methods in landslide investigations, *Engineering Geology*, 29, 59-78.
40. Nakamura Y., (1989) A method for dynamic characteristics estimation of subsurface using microtremor on the ground surface, *Quarterly Report of the Railway Technical Research Institute*, 30, 25-33.
41. Neseftioglu H.A., Gokceoglu C., (2011) Probabilistic risk assessment in medium scale for rainfall-induced earth flows: Cataklic atachment area (Cayeli, Rize Turkey), *Mathematical Problems in Engineering*, 21.
42. Okay A.I., Sahinturk O., (1997) Geology of the eastern Pontides. In: Robinson AG (ed), regional and Petroleum Geology of the Black Sea and Surrounding Region, *American Association of Petroleum Geologist (AAPG) Memoir*, 68, 291-311.
43. Onalp A., Tarhan F., Sevin  N., (1987) Doğu Karadeniz heyelanları analizi, dengeli yamaç tasarımı, TÜBİTAK MAG: 585.
44. Onalp A., (1991) Dogu Karadeniz heyelanlarının nedenleri, analizi ve kontrol olanakları, Türkiye 1. Ulusal Heyelan Sempozyumu, Bildiriler Kitabı, 85-96.
45. Ozsayar T., Pelin S., Gedikoglu A., (1981) Cretaceous in the eastern Pontides, *Karadeniz Technical University Journal of Earth Sciences*, 1, 65-74.
46. Perrone A., Iannuzzi A., Lappena V., Lorenzo P., Piscitelli S., Rizzo, E., Sdao F., (2004) High-resolution electrical imaging of the Varco d'Izzo earthflow (southern Italy), *Journal of Applied Geophysics*, 56, 17-29.
47. Perrone A., Lappena V., Piscitelli S., (2014) Electrical resistivity technique for landslide investigation. A review, *Earth Science Reviews*, 135, 65-82.
48. Rodriguez V.H.S., Midorikawa S., (2002) Applicability of the H/V Spectral Ratio of Microtremors in Assessing Site Effects on Seismic Motion, *Earthquake Engineering and Structural Dynamics*, 31, 261-279.
49. Sass O., Bell R., Glade T., (2008) Comparasion of GPR, 2D resistivity and traditional techniques for the subsurface exploration of the Oschingen landslide, SwabianAlb (Germany), *Geomorphology*, 93(1), 89-103.
50. Schmutz M., Albouy Y., Gu erin R., Maquaire O., Vassal J., Schott J.J., Desclo tres M., (2000) Joint electrical and time domain electromagnetism (TDEM) data inversion applied to the Super Sauze earthflow (France), *Surveys in Geophys*, 21(4), 371-390.

51. Sen C., (2007) Jurassic volcanism in the eastern Pontides, *Turkish Journal of Earth Sciences*, 16, 523-539.
52. Sheffer M., Oldenburg D., (2007) Three-dimensional modelling of streaming potential, *Geophys. J. International*, 169, 839–848.
53. Suto K., (2003) Microtremor Survey Method, Geophysical Monograph Series, SEG.
54. Tarhan F., (1991) Dogu Karadeniz Bölgesi heyelanlarına genel bir bakış, Türkiye 1. Ulusal Heyelan Sempozyumu, Bildiriler Kitabı, 38-63.
55. Tlas M., Asfahani J., (2007) A best-estimate approach for determining selfpotential parameters related to simple geometric shaped structures, *Pure Appl. Geophysics*, 164, 2313–2328.
56. Wishart D., Slater L., Gates E., (2006) Self potential improves characterization of hydraulically-active fractures from azimuthal geoelectrical measurement, *Geophys. Res. Letters*, 33, L17314.
57. Yalcin A., Bulut F., (2007) Landslide susceptibility mapping using GIS and digital photogrammetric techniques: a case study from Ardesen (NE-Turkey), *Natural Hazards*, 41, 137-158.